

DESY 04-099
 TTP04-10
 UB-ECM-PF-04-16
 June 2004

Spin Dependence of Heavy Quarkonium Production and Annihilation Rates: Complete Next-to-Next-to-Leading Logarithmic result

A.A. Penin^{a,b}, A. Pineda^c, V.A. Smirnov^{d,e}, M. Steinhauser^e

^a *Institut für Theoretische Teilchenphysik, Universität Karlsruhe,
 76128 Karlsruhe, Germany*

^b *Institute for Nuclear Research, Russian Academy of Sciences,
 60th October Anniversary Prospect 7a, 117312 Moscow, Russia*

^c *Dept. d'Estructura i Constituents de la Matèria, U. Barcelona,
 Diagonal 647, E-08028 Barcelona, Catalonia, Spain*

^d *Institute for Nuclear Physics, Moscow State University,
 119992 Moscow, Russia*

^e *II. Institut für Theoretische Physik, Universität Hamburg,
 Luruper Chaussee 149, 22761 Hamburg, Germany*

Abstract

The ratio of the photon mediated production or annihilation rates of spin triplet and spin singlet heavy quarkonium states is computed to the next-to-next-to-leading logarithmic accuracy within the nonrelativistic renormalization group approach. The result is presented in analytical form and applied to the phenomenology of $t\bar{t}$, $b\bar{b}$ and $c\bar{c}$ systems. The use of the nonrelativistic renormalization group considerably improves the behaviour of the perturbative expansion and is crucial for accurate theoretical analysis. For bottomonium decays we predict $\Gamma(\eta_b(1S) \rightarrow \gamma\gamma) = 0.659 \pm 0.089(\text{th.})^{+0.019}_{-0.018}(\delta\alpha_s) \pm 0.015(\text{exp.})$ keV. Our results question the accuracy of the existing extractions of the strong coupling constant from the bottomonium annihilation. As a by-product we obtain novel corrections to the ratio of the ortho- and parapositronium decay rates: the corrections of order $\alpha^4 \ln^2 \alpha$ and $\alpha^5 \ln^3 \alpha$.

PACS numbers: 12.38.Cy, 13.20.Gd

1 Introduction

Annihilation of a heavy quarkonium into leptons, photons or light hadrons, as well as its production in e^+e^- or $\gamma\gamma$ collisions, has been a subject of numerous investigations starting from earliest applications of perturbative quantum chromodynamics (QCD) [1] and has by now become a classical problem. The annihilation of the nonrelativistic bound state possesses a highly sophisticated multi-scale dynamics and, not surprisingly, was the original testing ground for the effective field theory of nonrelativistic QCD (NRQCD) [2,3]. On the phenomenological side, the ratio of the bottomonium annihilation rates into leptons and light hadrons is currently used to determine the value of the strong coupling constant α_s [4]. Furthermore, the study of $t\bar{t}$ threshold production at a future Linear Collider could even allow us to probe Higgs-boson-induced effects [5]. The calculation of the high-order QCD corrections is mandatory to provide accurate theoretical predictions for the production and annihilation rates, however, this is a challenging theoretical problem. For most of the channels, the perturbative corrections are only known to one-loop accuracy [6]. The complete $\mathcal{O}(\alpha_s^2)$ correction is known only for the one- and two-photon mediated processes [7,8,9,10,11,12,13,14]. The perturbative series, however, shows a slow convergence and the results suffer from a rather strong dependence on the normalization scale ν of $\alpha_s(\nu)$. The resummation of the large logarithms of the heavy quark velocity to all orders in α_s has been advocated as a tool to improve the behaviour of the perturbative expansion for $t\bar{t}$ threshold production [15]. Currently, the complete next-to-leading logarithmic (NLL) approximation for the production and annihilation rates is available [16,17]. The first attempt to go beyond the NLL approximation [15] suggested a very good convergence of the logarithmic expansion. In particular, an accuracy of 2-3% was claimed for the cross section of $t\bar{t}$ threshold production. However, subsequent calculations of some next-to-next-to-leading logarithmic (NNLL) terms [18], which had not been taken into account in Ref. [15], casted serious doubts on this optimistic estimate. Thus, the full calculation of the NNLL corrections, which still remains elusive, is unavoidable to draw definite conclusions.

In this paper we derive the *complete* NNLL result for the spin dependent part of the heavy quarkonium production annihilation rates which includes the terms of the form $\alpha_s^{n+2} \ln^n \alpha_s$ for all n . The structure of the paper is as follows. In the next section we recall the basic ingredients of the effective theory description of the production and annihilation rates. In Sect. 3 we derive the nonrelativistic renormalization group (NRG) equation and in Sect. 4 we present its solution. The result is applied to $t\bar{t}$ threshold production, bottomonium and charmonium phenomenology in Sect. 5. Sect. 6 contains our conclusions. Explicit results for the potentials and the analytical solution of the equations are given in Appendices A and B, respectively. Appendix C includes the new results for the high-order logarithmic corrections to the positronium decay rates.

2 Effective theory description of the production and annihilation rates

The perturbative dynamics of the nonrelativistic bound state is characterised by three well separated scales: the heavy quark mass m_q (the hard scale), the bound state momentum vm_q (the soft scale), and the bound state energy v^2m_q (the ultrasoft scale), where $v \propto \alpha_s \ll 1$ is the velocity of the nonrelativistic heavy quark for the approximately Coulombic bound state. A systematic evaluation of the corrections to the bound state parameters is based on the effective field theory concept of the scale separation [2], which is at the heart of the recent progress in the perturbative QCD bound-state calculations.

The one-photon mediated processes are induced by the electromagnetic current j_μ . Its space components have the following decomposition in terms of operators constructed from the nonrelativistic quark and antiquark two-component Pauli spinors ψ and χ [3]:

$$\mathbf{j} = c_v(\nu) \psi^\dagger \boldsymbol{\sigma} \chi + \frac{d_v(\nu)}{6m_q^2} \psi^\dagger \boldsymbol{\sigma} \mathbf{D}^2 \chi + \dots, \quad (1)$$

where ν is the renormalization scale, \mathbf{D} is the covariant derivative, $\boldsymbol{\sigma}$ is the Pauli matrix, and the ellipsis stands for operators of higher mass dimension. The Wilson coefficients c_v and d_v represent the contributions from the hard modes and may be evaluated as a series in α_s in full QCD for free on-shell on-threshold external (anti)quark fields. We define it through

$$c_v(\nu) = \sum_{i=0}^{\infty} \left(\frac{\alpha_s(\nu)}{\pi} \right)^i c_v^{(i)}(\nu) , \quad c_v^{(0)} = 1 , \quad (2)$$

and similarly for other coefficients.

The operator responsible for the two-photon S -wave processes in the nonrelativistic limit is generated by the expansion of the product of two electromagnetic currents and has the following representation [3]

$$O_{\gamma\gamma} = c_{\gamma\gamma}(\nu) \psi^\dagger \chi + \frac{d_{\gamma\gamma}(\nu)}{6m_q^2} \psi^\dagger \mathbf{D}^2 \chi + \dots, \quad (3)$$

which reduces to the pseudoscalar current in the nonrelativistic limit. The one-loop corrections to the hard coefficients are known for quite a long time [19,20]

$$\begin{aligned} c_v^{(1)} &= -2C_F , \\ c_{\gamma\gamma}^{(1)} &= -\left(\frac{5}{2} - \frac{\pi^2}{8}\right) C_F , \end{aligned} \quad (4)$$

where $C_F = (N_c^2 - 1)/(2N_c)$, $N_c = 3$. Let us define the spin ratio for the production and annihilation of heavy quarkonium \mathcal{Q} as

$$\mathcal{R}_q = \frac{\sigma(e^+e^- \rightarrow \mathcal{Q}(n^3S_1))}{\sigma(\gamma\gamma \rightarrow \mathcal{Q}(n^1S_0))} = \frac{\Gamma(\mathcal{Q}(n^3S_1) \rightarrow e^+e^-)}{\Gamma(\mathcal{Q}(n^1S_0) \rightarrow \gamma\gamma)} . \quad (5)$$

The effective theory expression for the spin ratio reads

$$\mathcal{R}_q = \frac{c_s^2(\nu)}{3Q_q^2} \frac{|\psi_n^v(0)|^2}{|\psi_n^p(0)|^2} + \mathcal{O}(v^4), \quad (6)$$

where Q_q is the quark electric charge, $c_s(\nu) = c_v(\nu)/c_{\gamma\gamma}(\nu)$, $\psi_n^{(v,p)}(\mathbf{r})$ are the spin triplet (vector) and spin singlet (pseudoscalar) quarkonium wave functions of the principal quantum number n . The wave functions describe the dynamics of the nonrelativistic bound state and can be computed within potential NRQCD (pNRQCD) [21]. The latter is the Schrödinger-like effective theory of potential (anti)quarks whose energy scales like $m_q v^2$ and three-momentum scales like $m_q v$, and their multipole interaction to the ultrasoft gluons [22,23]. The contributions of hard and soft modes in pNRQCD are represented by the perturbative and relativistic correction to the effective Hamiltonian, which is systematically evaluated order by order in α_s and v around the leading order (LO) Coulomb approximation. The LO Coulomb wave function reads $|\psi_n^C(0)|^2 = C_F^3 \alpha_s^3 m_q^3 / (8\pi n^3)$. Let us define

$$\frac{|\psi_n^v(0)|^2}{|\psi_n^p(0)|^2} = \rho_n(\nu) = \sum_{i=0}^{\infty} \left(\frac{\alpha_s(\nu)}{\pi} \right)^i \rho_n^{(i)}(\nu), \quad \rho_n^{(0)} = 1. \quad (7)$$

The next-to-leading (NLO) contribution $\rho_n^{(1)}$ vanishes since the corrections to the wave functions are spin-independent at this order.

Starting from $\mathcal{O}(\alpha_s^2)$, the hard coefficients are infrared (IR) divergent. This spurious divergence arises in the process of scale separation and is canceled against the ultraviolet (UV) one of the effective-theory result for the wave function at the origin. A powerful approach to deal with such divergences has been developed in Refs. [24,25,26]. It is based on dimensional regularization and the interpretation of the formal expressions derived from the Feynman rules of the effective theory in the sense of the threshold expansion [27,28]. This provides a factorization of the contributions from different scales. In the $\overline{\text{MS}}$ scheme the two-loop corrections to c_v are known in analytical form and given by [8,9]

$$\begin{aligned} [c_v^{(2)}(\nu)]^{\overline{\text{MS}}} = & \left(-\frac{151}{72} + \frac{89\pi^2}{144} - \frac{5\pi^2}{6} \ln 2 - \frac{13}{4} \zeta(3) \right) C_A C_F + \left(\frac{23}{8} - \frac{79\pi^2}{36} \right. \\ & \left. + \pi^2 \ln 2 - \frac{1}{2} \zeta(3) \right) C_F^2 + \left(\frac{22}{9} - \frac{2\pi^2}{9} \right) C_F T_F \\ & + \frac{11}{18} C_F T_F n_l + \left[\beta_0 + \pi^2 \left(\frac{C_A}{2} + \frac{C_F}{3} \right) \right] C_F \ln \left(\frac{m_q}{\nu} \right), \end{aligned} \quad (8)$$

where $\beta_0 = 11C_A/3 - 4n_l T_F/3$, $C_A = N_c$, $T_F = 1/2$, n_l is the number of light-quark flavours, $\zeta(3) = 1.202057\dots$ is the value of Riemann's ζ function, and α_s is renormalized in the $\overline{\text{MS}}$ scheme. For the two-photon processes the two-loop correction is known in semi-numerical form [14]

$$[c_{\gamma\gamma}^{(2)}(\nu)]^{\overline{\text{MS}}} = -4.79(5) C_A C_F - 21.02(10) C_F^2 + 0.224(1) C_F T_F + \left(\frac{41}{36} - \frac{13\pi^2}{144} - \frac{2}{3} \ln 2 \right)$$

$$-\frac{7}{24}\zeta(3)\Big)C_FT_Fn_l+\left[\left(\frac{5}{4}-\frac{\pi^2}{16}\right)\beta_0+\pi^2\left(\frac{C_A}{2}+C_F\right)\right]C_F\ln\left(\frac{m_q}{\nu}\right), \quad (9)$$

where the $gg \rightarrow \gamma\gamma$ contribution induced by a light-fermion box was estimated to be small and was not included in the result. Note that the above result depends on the definition of the nonrelativistic axial current. The next-to-next-to-leading (NNLO) correction to the wave functions ratio in $\overline{\text{MS}}$ scheme reads [14,29]

$$\left[\rho_n^{(2)}(\nu)\right]^{\overline{\text{MS}}} = \frac{2}{3}\pi^2C_F^2\left[-\frac{7}{3}+2\Psi_1(n)+2\gamma_E-\frac{2}{n}+2\ln\left(\frac{C_F\alpha_s(\nu)m_q}{n\nu}\right)\right]. \quad (10)$$

where $\Psi_n(x) = d^n \ln \Gamma(x)/dx^n$, $\Gamma(z)$ is Euler's Γ function, and $\gamma_E = 0.577216\dots$ is Euler's constant. However, for the renormalization group analysis it is more convenient to use the *hard matching* scheme where the nonlogarithmic part of the divergent two-loop potential-potential contribution, which appears in the time-independent perturbation theory for the nonrelativistic wave function, is shifted to the hard coefficient. The NNLO corrections in this scheme are obtained from the $\overline{\text{MS}}$ result by the following shift

$$\hat{\rho}_n^{(2)} = \left[\rho_n^{(2)}\right]^{\overline{\text{MS}}} + \frac{14}{9}\pi^2C_F^2, \quad \hat{c}_s^{(2)} = \left[c_s^{(2)}\right]^{\overline{\text{MS}}} - \frac{7}{9}\pi^2C_F^2. \quad (11)$$

3 Renormalization group evolution of c_s

In general, the logarithmic corrections originate from logarithmic integrals over virtual momenta ranging between the scales and reveal themselves as the singularities of the effective theory couplings. The renormalization of these singularities allows one to derive the equations of the NRG, which describe the running of the effective theory couplings (Wilson coefficients), *i.e.* their dependence on the effective theory cutoffs. The solution of these equations sums up the logarithms of the scale ratios. To derive NRG equations necessary for the NNLL analysis of the decay rates we rely on the method developed in Ref. [16] where, in particular, the correct NLL result for the decay rates has been obtained for the first time (see also Ref. [17]). The NRG equations express the dependence of the effective theory coupling constants on the IR cutoff. However, they are derived by studying the UV divergences of the effective theory perturbative expressions. In general, one has to consider the soft, potential and ultrasoft running of the effective theory coupling constants. We denote the corresponding cutoffs as ν_s , ν_p and ν_{us} , respectively. The soft running is associated with the divergences of the NRQCD perturbation theory for the potential while the potential running corresponds to the divergences of the time-independent perturbation theory for the nonrelativistic Green function in pNRQCD. As it was first realized in Ref. [30], ν_{us} and ν_p are correlated and the relation between them can be given by $\nu_{us} = \nu_p^2/m_q$. The matching to the hard contribution is performed at a generic scale $\nu_h \sim m_q$.

To NNLL approximation the hard coefficient c_s itself has only potential running. We compute the corresponding anomalous dimensions by inspecting the UV singular behaviour of the three-loop effective theory diagrams computed in Refs. [31,29] (see also

[32,33,34]). The NRG equation in the hard matching scheme is found to be

$$\frac{d \ln \hat{c}_s(\nu)}{d \ln \nu} = \frac{C_F^2}{3} \left[2\alpha_{V_s}(\nu) D_{S^2,s}^{(2)}(\nu) + \alpha_s(\nu) \frac{d D_{S^2,s}^{(2)}(\nu)}{d \ln \nu} \right]. \quad (12)$$

Here $\alpha_{V_s}(\nu) = \alpha_s(\nu) + \dots$ is the strong coupling constant defined through the perturbative potential between the static quark and antiquark in colour-singlet state

$$V_C(\mathbf{k}^2) = \frac{4\pi C_F \alpha_{V_s}(\mathbf{k}^2)}{\mathbf{k}^2}, \quad (13)$$

and $D_{S^2,s}^{(2)}(\nu) = \alpha_s(\nu) + \dots$ is the Wilson coefficient of the spin-flip potential in pNRQCD Hamiltonian

$$V_{S^2}^{(2)}(\nu_p, \nu_s) = \frac{4\pi \mathbf{S}^2 C_F D_{S^2,s}^{(2)}(\nu_p, \nu_s)}{3m_q^2}, \quad (14)$$

with $\mathbf{S} = (\boldsymbol{\sigma}_1 + \boldsymbol{\sigma}_2)/2$ being the total spin operator. In Eq. (12) we combine the soft and potential running by setting $\nu_s = \nu_p = \nu$, which is consistent to the order of interest. Note that the scheme used in this paper differs from the standard one used for the evaluation of the Feynman integrals in dimensional regularization in Ref. [29].

Let us now discuss the structure of the NRG equation (12) in more detail. The first term on the right-hand side originates from the diagram (a) in Fig. 1. The leading logarithmic (LL) soft running of α_{V_s} and $D_{S^2,s}^{(2)}$ is responsible for the NLL evolution of c_s . To get the NNLL result for the hard coefficient we need the NLL running of this quantities. The one of α_{V_s} is well known and can be found *e.g.* in Ref. [16]. For $D_{S^2,s}^{(2)}$ it has been recently obtained in Refs. [35,36]. The analytical result for the NLL evolution of the spin-flip potential is presented in Ref. [36] where, however, some details of the analysis have been skipped. This gap is filled in Appendix A, where explicit results for the contributing potentials are presented.

The second term on the right-hand side of Eq. (12) originates from the diagram (b) of Fig. 1. It starts to contribute to c_s at NNLL. Thus the LL expression for $D_{S^2,s}^{(2)}(\nu)$ can be used, which is given by [16,37]

$$\frac{d}{d \ln \nu} D_{S^2,s}^{(2)}(\nu) = \frac{\alpha_s^2(\nu)}{\pi} \gamma_s^{(1)} c_F^2(\nu), \quad \gamma_s^{(1)} = -\frac{\beta_0}{2} + \frac{7}{4} C_A. \quad (15)$$

c_F is the effective Fermi coupling, which is needed with LL accuracy, and reads $c_F(\nu_h) = z^{-C_A}$, where $z = (\alpha_s(\nu)/\alpha_s(\nu_h))^{1/\beta_0}$.

The initial condition for the NNLL solution of the NRG evolution is fixed by the two-loop value of $c_s(\nu_h)$ at a hard matching scale $\nu_h \sim m_q$. The subsequent evolution of $c_s(\nu)$ down to $\nu \sim \alpha_s m_q$ resums the logarithms of the coupling constant. The form of the NRG equation and the matching conditions is scheme dependent. A change of the scheme $\hat{c}_s^{(2)}(\nu_h) \rightarrow c_s^{(2)}(\nu_h) = \hat{c}_s^{(2)}(\nu_h) - \delta c_s \pi^2 C_F^2$ requires an additional full derivative term to be

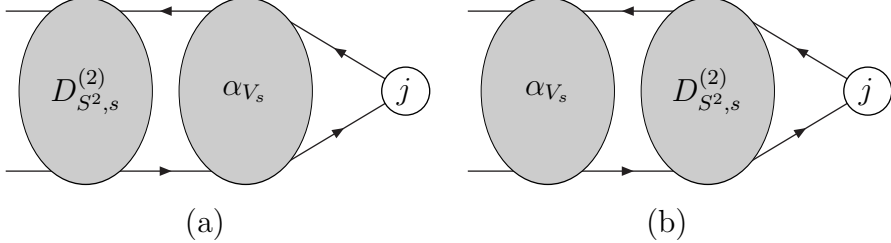


Figure 1: The pNRQCD diagrams contributing to the NNLL running of c_s . The shaded oval represents the soft running of the spin-flip or Coulomb potential and j is nonrelativistic vector or pseudoscalar current.

added to the right hand side of Eq. (12)

$$\delta c_s C_F^2 \frac{d}{d \ln \nu} (\alpha_{V_s}(\nu) D_{S^2,s}^{(2)}(\nu)) = \delta c_s C_F^2 \frac{\alpha_s^2(\nu)}{\pi} \left(-\frac{\beta_0}{2} D_{S^2,s}^{(2)}(\nu) + \gamma_s^{(1)} \alpha_s(\nu) c_F^2(\nu) \right) + \dots, \quad (16)$$

where δc_s specifies the scheme and the ellipses indicated higher orders in α_s . In particular we have $[\delta c_s]^{\overline{\text{MS}}} = -7/9$. Note that the coupling c_F appears in Eq. (12) in combination with the factor $\gamma_s^{(1)}$.

To get the NNLL approximation for the production and annihilation rates we formally have to take into account also the LL running of d_v and $d_{\gamma\gamma}$. These hard coefficients, however, have identical LL ultrasoft running which cancels out in the spin ratio.

4 Solution of the renormalization group equation

The solution of the renormalization group equation (12) is of the following form

$$\hat{c}_s(\nu) = \hat{c}_s(\nu_h) e^{\alpha_s(\nu_h) \Gamma_{\hat{c}_s}^{\text{NNLL}}(\nu) + \alpha_s^2(\nu_h) \Gamma_{\hat{c}_s}^{\text{NNLL}}(\nu) + \dots}. \quad (17)$$

The expression of $\Gamma_{\hat{c}_s}^{\text{NNLL}}$ is known [16,17]

$$\Gamma_{\hat{c}_s}^{\text{NNLL}}(\nu) = \frac{2\pi C_F^2 (2\beta_0 - 7C_A)}{3(\beta_0 - 2C_A)^2} (1 - z^{\beta_0 - 2C_A}) - \frac{2\pi C_F^2 C_A}{\beta_0(\beta_0 - 2C_A)} \ln(z^{\beta_0}). \quad (18)$$

The result for the NNLL function can also be obtained analytically¹ and can be cast in the form

$$\Gamma_{\hat{c}_s}^{\text{NNLL}}(\nu) = \pi^2 \sum_{i=1}^{19} A_i f_i(z), \quad (19)$$

¹For the practical calculation we use $\nu_{us} = \nu^2/\nu_h$, which is sufficient for the accuracy of our calculation.

where the coefficients A_i and functions $f_i(z)$ are given in Appendix B. To get the NNLL approximation for the spin ratio one has to take into account the NNLL contribution to the wave function, which is given by

$$\rho_n^{\text{NNLL}}(\nu) = 1 + \frac{1}{\pi^2} \left(\alpha_{V_s}(\nu) D_{S^2,s}^{(2)}(\nu) \right)^{\text{LL}} \hat{\rho}_n^{(2)}(\nu). \quad (20)$$

It cancels the NLL ν -dependence of c_s . Eqs. (17) and (20) give the NNLL approximation to the spin ratio. By expanding the resummed expression we reproduce the known results for the $\mathcal{O}(\alpha_s^2)$ [14], $\mathcal{O}(\alpha_s^3 \ln^2 \alpha_s)$ [31], and $\mathcal{O}(\alpha_s^3 \ln \alpha_s)$ [29] terms. After including the one-photon annihilation contribution, the Abelian part of our result reproduces the spin-dependent corrections of order $\alpha^3 \ln \alpha$ to the positronium decay rates [32,34]. The use of the NRG allows us to derive the higher order logarithmic corrections for positronium. The explicit results for the $\mathcal{O}(\alpha^4 \ln^2 \alpha)$ and $\mathcal{O}(\alpha^5 \ln^3 \alpha)$ terms are given in Appendix C.

5 Heavy quarkonium phenomenology

For the numerical estimates, we take $m_c = 1.5$ GeV, $m_b = M(\Upsilon)/2$ and $m_t = 175$ GeV, which is sufficient at the order of interest. Furthermore, we take $\alpha_s(M_Z)$ as an input and run with four-loop accuracy down to the matching scale ν_h to ensure the best precision. Below the matching scale, the running of α_s is used according to the logarithmic precision of the calculation in order not to include the corrections beyond the NNLL accuracy. By the same reason we expand the decay rates ratio in $\alpha_s(\nu_h)$ up to the NNLL accuracy. In Figs. 2, 3 and 4, the spin ratio is plotted as a function of ν in the various logarithmic and fixed-order approximations for the (hypothetical) toponium, bottomonium and charmonium ground states, respectively. As we see, in the second order the convergence and stability of the result with respect to the scale variation is substantially improved if one switches from the fixed-order to the logarithmic expansion. We want to remark that the ν dependence of the NLL approximation is slightly worse than at NLO. This is due to the artificially small ν dependence at NLO which is likely due to the fact that at this order only the hard scale enters.

Let us first consider the top quark case. The relatively large top quark width smears out the Coulomb-like poles below the threshold leaving a single well-pronounced resonance with the properties mainly determined by the “would be” toponium ground state parameters. Thus our result can be applied to the ratio of the cross sections of the resonance $e^+e^- \rightarrow t\bar{t}$ and $\gamma\gamma \rightarrow t\bar{t}$ production. As one can see in Fig. 2 the logarithmic expansion shows perfect convergence and the NNLL correction vanishes at the scale $\nu \approx 13$ GeV, which is close to the physically motivated scale of the inverse Bohr radius $\alpha_s m_t/2$. For illustration, at the scale of minimal sensitivity, $\nu = 20.2$, GeV we have

$$\frac{\sigma_{\text{res}}(e^+e^- \rightarrow t\bar{t})}{\sigma_{\text{res}}(\gamma\gamma \rightarrow t\bar{t})} = \frac{1}{3Q_t^2} (1 - 0.132 - 0.018). \quad (21)$$

Note that the perturbative expansion for the ground state energy, which is known to $\mathcal{O}(\alpha_s^3)$ [38], shows a similar nice property. However, it is not clear if the nice behaviour

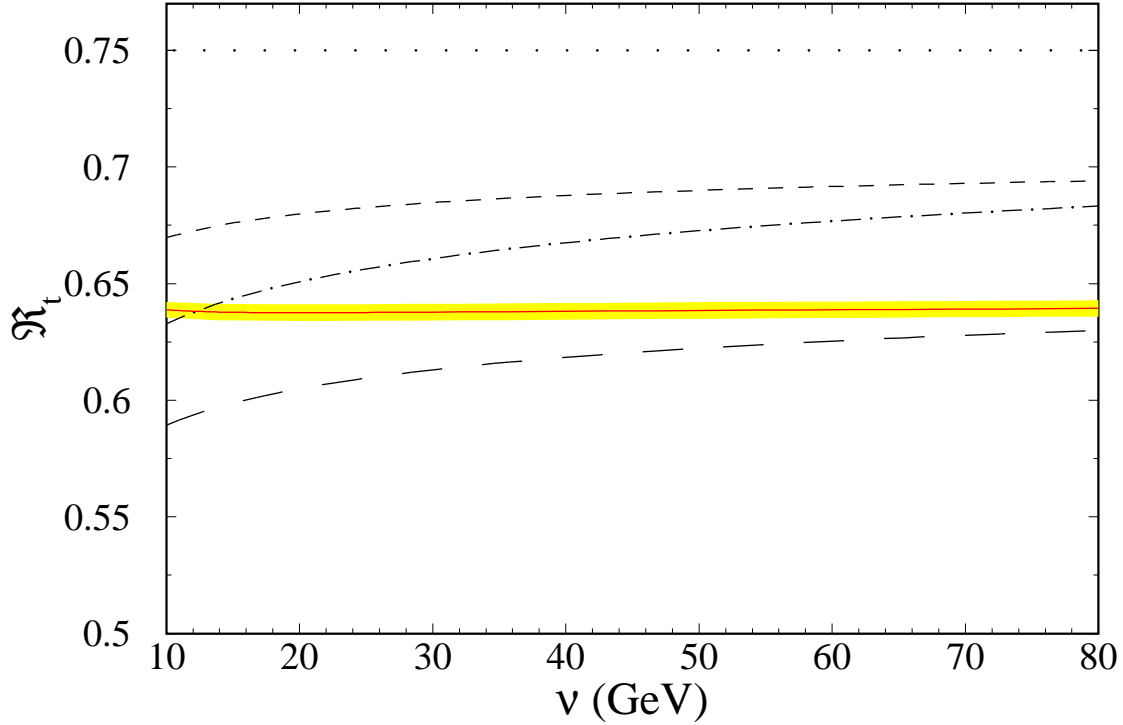


Figure 2: The spin ratio as the function of the renormalization scale ν in LO \equiv LL (dotted line), NLO (short-dashed line), NNLO (long-dashed line), NLL (dot-dashed line), and NNLL (solid line) approximation for the (would be) toponium ground state with $\nu_h = m_t$. For the NNLL result the band reflects the errors due to $\alpha_s(M_Z) = 0.118 \pm 0.003$. Note that for the vertical axis the zero is suppressed.

of the logarithmic expansion also holds for the spin-independent part of the threshold cross section. A possible problem is connected to the ultrasoft contribution, which is enhanced by the larger value of α_s at the ultrasoft scale. Whereas it is suppressed in the spin ratio by the fifth power of α_s , for the spin-independent part it already contributes at $\mathcal{O}(\alpha_s^3)$ and can destabilize the expansion.

For bottomonium, the logarithmic expansion shows nice convergence and stability (c.f. Fig. 3) despite the presence of ultrasoft contributions with α_s normalized at a rather low scale ν^2/m_b . At the same time, the perturbative corrections are important and reduce the leading order result by approximately 41%. For illustration, at the scale of minimal sensitivity, $\nu = 1.295$ GeV, we have the following series:

$$\frac{\Gamma(\Upsilon(1S) \rightarrow e^+e^-)}{\Gamma(\eta_b(1S) \rightarrow \gamma\gamma)} = \frac{1}{3Q_b^2} (1 - 0.302 - 0.111) . \quad (22)$$

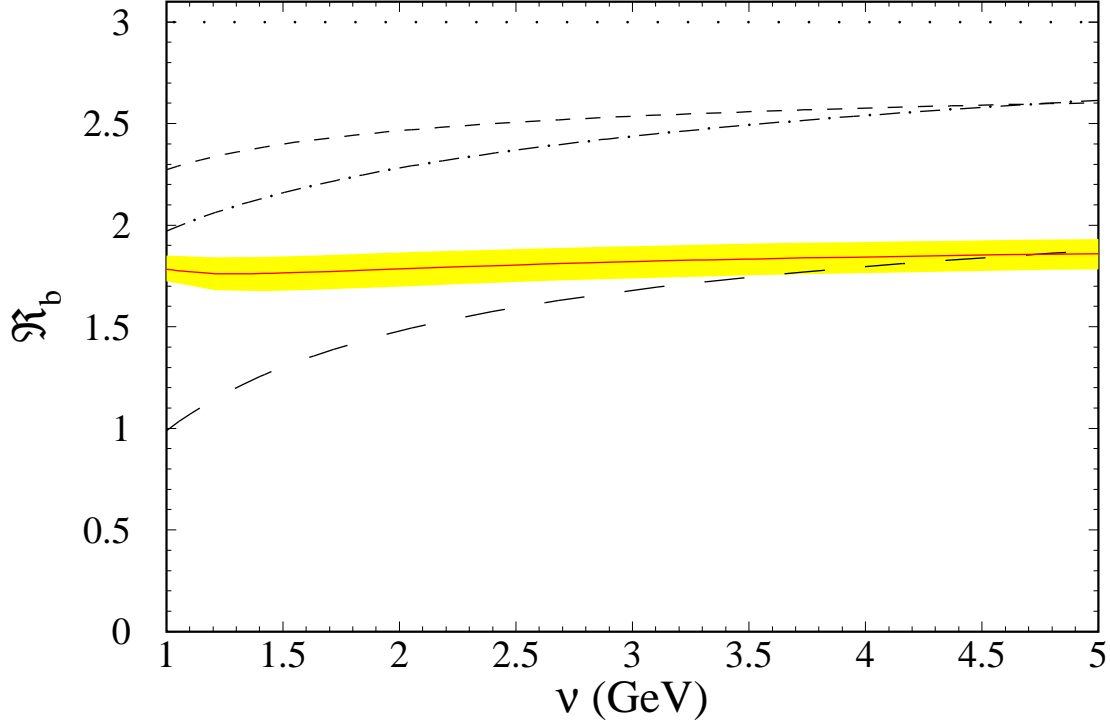


Figure 3: The spin ratio as the function of the renormalization scale ν in LO \equiv LL (dotted line), NLO (short-dashed line), NNLO (long-dashed line), NLL (dot-dashed line), and NNLL (solid line) approximation for the bottomonium ground state with $\nu_h = m_b$. For the NNLL result the band reflects the errors due to $\alpha_s(M_Z) = 0.118 \pm 0.003$.

In contrast, the fixed-order expansion blows up at the scale of the inverse Bohr radius.

So far we have discussed the perturbative corrections to the Coulomb-like quarkonium. However, in contrast to the $t\bar{t}$ system, for bottomonium nonperturbative contributions can be important. In our case the interaction of the quark-antiquark pair to the nonperturbative gluonic field is suppressed by ν through the multipole expansion. In every order of the multipole expansion the nonperturbative contribution is given by the convolution of the quantum mechanical Green function with a nonlocal nonperturbative gluonic correlator. In general, we know little about the structure of these quantities. If $\nu^2 m_q \gg \Lambda_{QCD}$, it can be investigated by the method of vacuum condensate expansion [39,40]. The resulting series, however, is not expected to converge well in our case and suffers from large numerical uncertainties [41,42]. Nevertheless, it is possible to estimate the nonrelativistic suppression of the leading nonperturbative effect. For the ratio of the decay rates the nonperturbative contribution emerges via the $\mathcal{O}(v^4)$ chromomagnetic dipole interaction

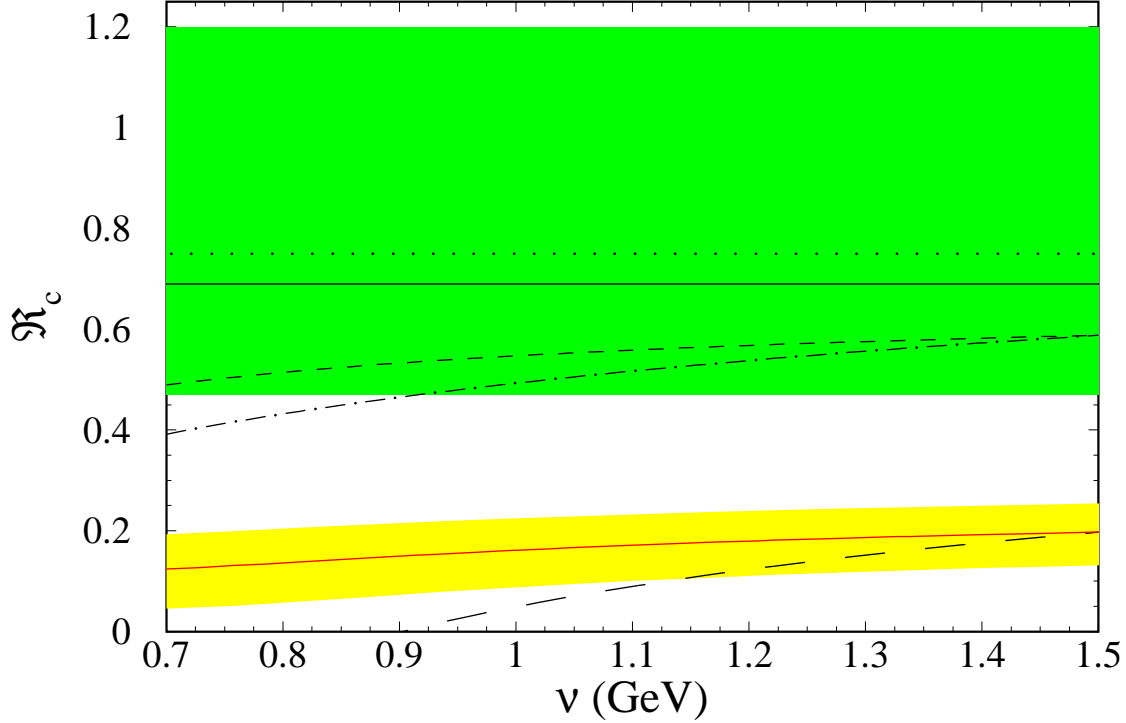


Figure 4: The spin ratio as the function of the renormalization scale ν in LO \equiv LL (dotted line), NLO (short-dashed line), NNLO (long-dashed line), NLL (dot-dashed line), and NNLL (solid line) approximation for the charmonium ground state with $\nu_h = m_c$. For the NNLL result the lower (yellow) band reflects the errors due to $\alpha_s(M_Z) = 0.118 \pm 0.003$. The upper (green) band represents the experimental error of the ratio [4] where the central value is given by the horizontal solid line.

and the interference between the $\mathcal{O}(v^2)$ chromoelectric dipole interaction and the leading $\mathcal{O}(v^2)$ spin-flip Fermi potential. Hence it is suppressed by the factor v^4 . Within the power counting assumed in this paper it only contributes in the N⁴LL approximation, far beyond the precision of our computation. Note that the nonperturbative contribution to the decay rates ratio is suppressed by a factor v^2 in comparison to the binding energy and decay rates, where the leading nonperturbative effect is due to chromoelectric dipole interaction. Thus the renormalization group improved result allows for very accurate theoretical evaluation of the spin ratio and, by using the available experimental data on the Υ meson as input, we can predict the production and annihilation rates of the yet undiscovered η_b meson with high precision. In particular, we predict the $\eta_b(1S)$ decay

rate using the experimental value for the $\Upsilon(1S)$ decay rate

$$\Gamma(\eta_b(1S) \rightarrow \gamma\gamma) = 0.659 \pm 0.089(\text{th.})^{+0.019}_{-0.018}(\delta\alpha_s) \pm 0.015(\text{exp.}) \text{ keV}, \quad (23)$$

where we have taken $\nu = 1.295$ GeV, the scale of minimal sensitivity, for the central value, the difference between the NLL and NNLL result for the theoretical error and $\alpha_s(M_Z) = 0.118 \pm 0.003$. The last error in Eq. (23) reflects the experimental error of $\Gamma(\Upsilon(1S) \rightarrow e^+e^-) = 1.314 \pm 0.029$ keV [4]. This value considerably exceeds the result for the absolute value of the decay width obtained in Ref. [43] on the basis of the full NLL analysis including the spin-independent part. This can be a signal of slow convergence of the logarithmic expansion for the spin-independent contribution which is more sensitive to the dynamics of the bound state and in particular to the ultrasoft contribution as it has been discussed above. On the other hand, the renormalon effects [44] could produce some systematic errors in the pure perturbative evaluations of the production/annihilation rates. The problem is expected to be more severe for the charmonium case discussed below.

We would also like to remark that the one-loop result for $\nu = m_b$ overshoots the NNLL one by approximately 30%. This casts some doubts on the accuracy of the existing α_s determination from the $\Gamma(\Upsilon \rightarrow \text{light hadrons})/\Gamma(\Upsilon \rightarrow e^+e^-)$ decay rates ratio, which gives $\alpha_s(m_b) = 0.177 \pm 0.01$, well below the “world average” value [4]. The theoretical uncertainty in the analysis is estimated through the scale dependence of the one-loop result. Our analysis of the photon mediated annihilation rates indicates that the actual magnitude of the higher order corrections is most likely quite beyond such an estimate and the theoretical uncertainty given in [4] should be increased by a factor of two. This brings the result for α_s into 1σ distance from the “world average” value.

For the charmonium, the NNLO approximation becomes negative at an intermediate scale between $\alpha_s m_c$ and m_c (c.f. Fig. 4) and the use of the NRG is mandatory to get a sensible perturbative approximation. The NNLL approximation has good stability against the scale variation but the logarithmic expansion does not converge well. This is the main factor that limits the theoretical accuracy since the nonperturbative contribution is expected to be under control. For illustration, at the scale of minimal sensitivity, $\nu = 0.645$ GeV, we obtain

$$\frac{\Gamma(J/\Psi(1S) \rightarrow e^+e^-)}{\Gamma(\eta_c(1S) \rightarrow \gamma\gamma)} = \frac{1}{3Q_c^2} (1 - 0.513 - 0.326). \quad (24)$$

The central value of our NNLL result is 2σ below the experimental value. The discrepancy may be explained by the large higher order contributions. This should not be surprising because of the rather large value of α_s at the inverse Bohr radius of charmonium. For the charmonium hyperfine splitting, however, the logarithmic expansion converges well and the prediction of the NRG is in perfect agreement with the experimental data. Thus one can try to improve the convergence of the series for the production/annihilation rates by accurately taking into account the renormalon-related contributions. One point to note is that with a potential model evaluation of the wave function correction, the sign of the

NNLO term is reversed in the charmonium case [14]. At the same time the subtraction of the pole mass renormalon from the perturbative static potential makes explicit that the potential is steeper and closer to lattice and phenomenological potential models [45]. Therefore, the incorporation of higher order effects from the static potential may improve the agreement with experiment. In any case, if we estimate the theoretical uncertainty as the difference of the NNLL and the NLL result at the soft scale $\alpha_s m_c$, the theoretical and experimental values agree within the error bars.

6 Summary

To conclude, we have resummed to all orders in the perturbative expansion the next-to-next-to-leading logarithms in the ratio of the one-photon mediated production and annihilation rate of the spin-triplet heavy quarkonium state to the two-photon one of the spin-singlet state. This constitutes the first complete NNLL result for the production and annihilation of heavy quarkonia. The use of the NRG improves the convergence of the perturbative series and stabilizes the result with respect to the scale variation. This allows us to obtain extremely accurate predictions for the $t\bar{t}$ threshold production. However, we still cannot draw a definite conclusion about the accuracy of the NNLL approximation to the spin independent part of the threshold production cross section, which could be worse due to the ultrasoft contribution.

For the bottomonium case we found convergence of the logarithmic expansion at the physically motivated scale of inverse Bohr radius and very weak scale dependence of the NNLL approximation. Using these results we can give predictions for the yet to be discovered η_b meson two-photon production/annihilation rates. The magnitude of the higher order corrections questions the reported accuracy of α_s determination from the $\Gamma(\Upsilon \rightarrow \text{light hadrons})/\Gamma(\Upsilon \rightarrow e^+e^-)$ ratio based on the one-loop theoretical analysis.

For the charmonium annihilation the NRG is mandatory to bring physical sense to the perturbative result because the NNLO approximation becomes negative at an intermediate scale. Though the NNLL approximation has very good stability with respect to the scale variation, the convergence of the logarithmic expansion is slow and essentially limits the accuracy of the perturbative prediction. Taking into account the large uncertainties of our result and the experimental data there is agreement and a lower value for the ratio seems to be favoured by our result.

As a by-product of the heavy quarkonium analysis we have obtained novel results for positronium: the complete $O(\alpha^4 \ln^2 \alpha)$ and $O(\alpha^5 \ln^3 \alpha)$ corrections to the ratio of the ortho- and parapositronium decay rates.

Acknowledgments:

The work of A.A.P. was supported in part by BMBF Grant No. 05HT4VKA/3 and SFB Grant No. TR 9. The work of A.P. was supported in part by MCyT and Feder (Spain), FPA2001-3598, by CIRIT (Catalonia), 2001SGR-00065 and by the EU network EURIDICE, HPRN-CT2002-00311. The work of V.A.S. was supported in part by RFBR

Project No. 03-02-17177, Volkswagen Foundation Contract No. I/77788, and DFG Mercator Visiting Professorship No. Ha 202/1. M.S. was supported by HGF Grant No. VH-NH-008.

Appendix A: NRG evolution of the spin-flip potential

In order to obtain c_s to NNLL accuracy one needs the matching coefficient of the spin-flip potential, $D_{S^2,s}^{(2)}$, to NLL order, which has been considered in Ref. [36]. In this Appendix we provide additional details.

The soft running of $D_{S^2,s}^{(2)}$ to NLL approximation is discussed in detail in Ref. [36]. The NRG evolution of the spin-flip potential also includes the potential and ultrasoft running at NLL, which is described below. To compute the potential running, we inspect all operators that induce spin-dependent UV divergences in the time-independent perturbation theory contribution with one and two potential loops. They include

- (i) the tree-level $\mathcal{O}(v^4)$ operators,
- (ii) the one-loop $\mathcal{O}(\alpha_s v^3)$ operators, and
- (iii) the $\mathcal{O}(v^2, \alpha_s v)$ operators,

which we in turn discuss in the following. In Appendix A.4 we discuss the three-loop ultrasoft-potential contribution and, finally, in Appendix A.5 we provide the NRG equation for the potential running.

A.1 Tree-level potentials of order v^4

The operators relevant for our calculation read

$$V_{S^2,1}^{(4)} = \pi C_F \alpha_s \frac{c_S^{(1)} c_S^{(2)}}{4m_1^2 m_2^2} \frac{1}{\mathbf{k}^2} \boldsymbol{\sigma}_1 \cdot (\mathbf{k} \times \mathbf{p}) \boldsymbol{\sigma}_2 \cdot (\mathbf{k} \times \mathbf{p}), \quad (25)$$

$$V_{S^2,2}^{(4)} = -\pi C_F \alpha_s \frac{c_F^{(1)} c_F^{(2)}}{4m_1^2 m_2^2} \frac{(\mathbf{p}^2 - \mathbf{p}'^2)^2}{\mathbf{k}^2} \left(\boldsymbol{\sigma}_1 \cdot \boldsymbol{\sigma}_2 - \frac{\boldsymbol{\sigma}_1 \cdot \mathbf{k} \boldsymbol{\sigma}_2 \cdot \mathbf{k}}{\mathbf{k}^2} \right), \quad (26)$$

$$V_{S^2,3}^{(4)} = \pi C_F \alpha_s \frac{\mathbf{p}^2 - \mathbf{p}'^2}{2\mathbf{k}^2} \left[\frac{c_S^{(1)} c_F^{(2)}}{4m_1^3 m_2} (\boldsymbol{\sigma}_1 \times (\mathbf{p} + \mathbf{p}')) \cdot (\boldsymbol{\sigma}_2 \times \mathbf{k}) + (1 \leftrightarrow 2) \right], \quad (27)$$

$$\begin{aligned} V_{S^2,4}^{(4)} = & -\frac{\pi C_F \alpha_s}{8\mathbf{k}^2} \left[\frac{c_{pp'}^{(1)} c_F^{(2)}}{m_1^3 m_2} \boldsymbol{\sigma}_1 \cdot (\mathbf{p} + \mathbf{p}') \left(\boldsymbol{\sigma}_2 \cdot (\mathbf{p} + \mathbf{p}') \mathbf{k}^2 + (\mathbf{p}^2 - \mathbf{p}'^2) \boldsymbol{\sigma}_2 \cdot \mathbf{k} \right) \right. \\ & \left. + (1 \leftrightarrow 2) \right]. \end{aligned} \quad (28)$$

Here \mathbf{p} and $\mathbf{p}' = \mathbf{p} + \mathbf{k}$ are the momentum of incoming and outgoing quark, we consider the general case with quark and antiquark of different masses m_1 and m_2 , and adopt the

standard notations for the NRQCD coupling constants c_F , *etc.* (see, *e.g.* Ref. [46]). The operators in Eqs. (25)-(27) can be inferred from the analysis of the hyperfine splitting QED [25] with a trivial adjustment of the colour structure. Eq. (25) corresponds to Eq. (13) of Ref. [25]. The potential (26) results from the expansion of the transverse gluon propagator in the energy transfer up to k_0^2 with subsequent use of the Coulomb equation of motion [24]

$$k_0^2 = -\frac{(\mathbf{p}^2 - \mathbf{p}'^2)^2}{4m_1 m_2}. \quad (29)$$

It reproduces the retardation effect given by Eq. (32) of Ref. [25].

The potentials proportional to c_{SCF} appear both at tree and one-loop level. There are two c_S NRQCD vertices that contribute to our calculation. One of them is proportional to $A_0 \mathbf{A}$. It is responsible half of the contribution proportional to c_{SCF} in Eq. (30) of the next subsection. The other involves the time derivative $\partial_0 \mathbf{A}$. To compute this contribution we perform a field redefinition in the NRQCD Lagrangian which in the lowest order is equivalent to using the equations of motion. In this way we obtain two new vertices. The first vertex is proportional to $(\mathbf{p}^2/m)\mathbf{A}$ and produces the potential in Eq. (27), which agrees with the first term in Eq. (22) of Ref. [25]. The second vertex is proportional to $A_0 \mathbf{A}$ and is responsible for the second half of the c_{SCF} contribution of the one-loop operator in Eq. (30).

The potential (28) was not considered in Ref. [25] since in QED $c_{p'p} = \mathcal{O}(\alpha)$ and thus $V_{S^2,4}^{(4)}$ gives at most corrections of order α^3 to the hyperfine splitting. Moreover, in QED this potential contributes only to the NNLL running of the spin-flip operator as the coupling $c_{p'p}$ has no anomalous dimension. However, in QCD $c_{p'p}$ does run and we have to take it into account.

There also exist $\mathcal{O}(v^4)$ potentials including the product of $c_{W_2} c_F$ or $c_{W_1} c_F$. They are, however, proportional to $(\mathbf{p} \cdot \mathbf{p}')(\boldsymbol{\sigma}_1 \cdot \boldsymbol{\sigma}_2)$ and $(\mathbf{p}^2 + \mathbf{p}'^2)(\boldsymbol{\sigma}_1 \cdot \boldsymbol{\sigma}_2)$, respectively, which do not produce potential divergences to the order of interest.

To get the NLL approximation for the spin-flip potential we need the LL running of the $\mathcal{O}(v^4)$ potentials, which is determined by the soft running of the NRQCD coupling constants. They are either known [16] or can be deduced using reparameterization invariance [46].

A.2 One-loop potentials of order $\alpha_s v^3$

The operators relevant for our calculation are

$$\begin{aligned} V_{S^2}^{(3)} = & -\frac{1}{24}(\pi\alpha_s)^2 C_F (4C_F - C_A) \left(\frac{c_F^{(1)} c_S^{(2)}}{m_1 m_2^2} + \frac{c_S^{(1)} c_F^{(2)}}{m_1^2 m_2} \right) |\mathbf{k}| \boldsymbol{\sigma}_1 \cdot \boldsymbol{\sigma}_2 \\ & + \frac{1}{24}(\pi\alpha_s)^2 C_F C_A \frac{c_F^{(1)} c_F^{(2)}}{m_1 m_2} \frac{1}{|\mathbf{k}|} \left(\frac{\mathbf{p}^2 + \mathbf{p}'^2}{2m_r} - 2E - \frac{\mathbf{k}^2}{2m_r} \right) \boldsymbol{\sigma}_1 \cdot \boldsymbol{\sigma}_2 \\ & - \frac{1}{96}(\pi\alpha_s)^2 C_F C_A \left(\frac{c_F^{(1)} c_F^{(2)2}}{m_1 m_2^2} + \frac{c_F^{(1)2} c_F^{(2)}}{m_1^2 m_2} \right) |\mathbf{k}| \boldsymbol{\sigma}_1 \cdot \boldsymbol{\sigma}_2, \end{aligned} \quad (30)$$

where E is the two-particle energy. The Abelian piece reproduces Eq. (34) of Ref. [25] whereas the non-Abelian part is new. Note that the second line gives no NLL contribution as the term proportional to E develops no logarithm and the remaining two terms cancel each other. We need the NLL running of this potential, which is inherited through the LL soft running of the NRQCD coupling constants.

A.3 Double insertion of $\mathcal{O}(v^2, \alpha_s v)$ operators

The basis of the $\mathcal{O}(v^2, \alpha_s v)$ operators is well known from the lower order calculations and can, *e.g.* be found in Refs. [47,26]. To get the NLL contribution to the spin-flip potential from the double insertion of these operators we need the LL soft and ultrasoft running of the $\mathcal{O}(v^2)$ terms and NLL soft and ultrasoft running of $\mathcal{O}(\alpha_s v)$ operators, which are known for the equal mass case [16]. For the non-equal mass case, most of the results can be trivially generalized (c.f. Ref. [16]) except for $D_{d,s}^{(2)}$, which depends on the four-fermion couplings of NRQCD. Among these couplings only for d_{vs} a nontrivial change is necessary. The corresponding NRG equation can be found in Ref. [16] and its solution reads

$$\begin{aligned}
d_{vs}(\nu) = & d_{vs}(\nu_h) - \alpha_s(\nu_h) \left[4C_F - 3\frac{C_A}{2} - \frac{5}{4}C_A \left(\frac{m_1}{m_2} + \frac{m_2}{m_1} \right) \right] \frac{2\pi}{\beta_0} (z^{\beta_0} - 1) \\
& - \alpha_s(\nu_h) \left(\frac{m_1}{m_2} + \frac{m_2}{m_1} \right) \frac{27C_A^2}{9C_A + 8T_F n_l} \frac{\pi}{2\beta_0} \left\{ -\frac{5C_A + 4T_F n_l}{4C_A + 4T_F n_l} \right. \\
& \times \frac{\beta_0}{\beta_0 - 2C_A} (z^{\beta_0 - 2C_A} - 1) + \frac{C_A + 16C_F - 8T_F n_l}{2(C_A - 2T_F n_l)} (z^{\beta_0} - 1) \\
& + \frac{-7C_A^2 + 32C_A C_F - 4C_A T_F n_l + 32C_F T_F n_l}{4(C_A + T_F n_l)(2T_F n_l - C_A)} \\
& \times \frac{3\beta_0}{3\beta_0 + 4T_F n_l - 2C_A} (z^{\beta_0 + 4T_F n_l/3 - 2C_A/3} - 1) \\
& + \frac{8T_F n_l}{9C_A} \left[\frac{\beta_0}{\beta_0 - 2C_A} (z^{\beta_0 - 2C_A} - 1) + \left(\frac{20}{13} + \frac{32}{13} \frac{C_F}{C_A} \right) \right. \\
& \left. \times \left([z^{\beta_0} - 1] - \frac{6\beta_0}{6\beta_0 - 13C_A} [z^{\beta_0 - \frac{13C_A}{6}} - 1] \right) \right] \left. \right\}. \tag{31}
\end{aligned}$$

A.4 Three-loop ultrasoft-potential running

Another NLL contribution to the spin-flip potential comes from the three-loop NLL ultrasoft-potential running of a $\mathcal{O}(v^2)$ spin-flip operator. The contribution is related to the chromomagnetic dipole gluon exchange which generate the potential of the following form in the coordinate representation

$$V_{S^2,1/r^3}^{(2)} = \frac{4C_F \mathbf{S}^2}{3m_1 m_2} (V_o - V_s)^3 D_{S^2,1/r^3}^{(2)}, \tag{32}$$

where

$$\begin{aligned} V_s &= -C_F \frac{\alpha_s}{|\mathbf{r}|}, \\ V_o &= \left(\frac{C_A}{2} - C_F \right) \frac{\alpha_s}{|\mathbf{r}|}. \end{aligned} \quad (33)$$

The ultrasoft running of the potential is determined by the NRG equation

$$\frac{dV_{S^2,1/r^3}^{(2)}(\nu_{us})}{d \ln \nu_{us}} = \frac{\alpha_s}{\pi} \frac{2C_F}{3m_1m_2} (V_o - V_s)^3, \quad (34)$$

and the solution for the Wilson coefficient reads

$$D_{S^2,1/r^3}^{(2)}(\nu_{us}) = \frac{1}{\beta_0} \log \left(\frac{\alpha_s(1/|\mathbf{r}|)}{\alpha_s(\nu_{us})} \right). \quad (35)$$

The potential (32) is singular at $|\mathbf{r}| \rightarrow 0$ and should be understood as the Fourier transform of $\ln(|\mathbf{k}|/\nu_p)$.

A.5 NRG equation for potential running

With all the relevant operators at hand it is straightforward to derive the NRG equation for the NLL potential running of the spin-flip potential. It reads

$$\begin{aligned} \frac{dD_{S^2,s}^{(2)}}{d \ln \nu} &= -2m_r^3 \left(\frac{1}{m_1^3} + \frac{1}{m_2^3} \right) C_F^2 \alpha_{V_s}^2 D_{S^2,s}^{(2)} + \frac{m_r^2}{m_1 m_2} C_F^2 \alpha_{V_s} \left(2D_{d,s}^{(2)} D_{S^2,s}^{(2)} \right. \\ &\quad \left. + \frac{8}{3} (D_{S^2,s}^{(2)})^2 - 8D_{S^2,s}^{(2)} D_{1,s}^{(2)} - \frac{5}{12} (D_{S_{12,s}}^{(2)})^2 \right) - C_A C_F D_s^{(1)} D_{S^2,s}^{(2)} \\ &\quad + \frac{1}{2} \alpha_s^3 C_F^2 m_r^2 \left(\frac{c_{pp'}^{(1)}}{m_1^2} c_F^{(2)} + c_F^{(1)} \frac{c_{pp'}^{(2)}}{m_2^2} \right) - 2\alpha_s^3 C_F^2 \frac{m_r^2}{m_1 m_2} c_F^{(1)} c_F^{(2)} \\ &\quad - \frac{1}{4} \alpha_s^3 C_F^2 \frac{m_r^2}{m_1 m_2} c_S^{(1)} c_S^{(2)} - \alpha_s^3 C_F^2 m_r^2 \left(c_F^{(1)} \frac{c_S^{(2)}}{m_2^2} + \frac{c_S^{(1)}}{m_1^2} c_F^{(2)} \right) \\ &\quad + \frac{1}{2} \alpha_s^3 C_F (4C_F - C_A) m_r \left(c_F^{(1)} \frac{c_S^{(2)}}{m_2} + \frac{c_S^{(1)}}{m_1} c_F^{(2)} \right) \\ &\quad + \frac{1}{8} \alpha_s^3 C_F C_A m_r \left(c_F^{(1)} \frac{c_F^{(2)2}}{m_2} + \frac{c_F^{(1)2}}{m_1} c_F^{(2)} \right) - \frac{C_A^3 \alpha_s^3}{2} D_{S^2,1/r^3}^{(2)}, \end{aligned} \quad (36)$$

where $m_r = m_1 m_2 / (m_1 + m_2)$ is the reduced mass. The notation for the Wilson coefficients is adopted from Ref. [16], where also explicit results can be found. The first two lines of Eq. (36) correspond to the double insertion of the $\mathcal{O}(v^2, \alpha_s v)$ operators discussed in Appendix A.3. Note that the contribution proportional to $(D_{S_{12,s}}^{(2)})^2$ disagrees with the

result of Ref. [48]. To reproduce the $\mathcal{O}(\alpha^2)$ corrections to the positronium hyperfine splitting [49,25] in Ref. [48] the factor 9 of the corresponding Wilson coefficient U_t^2 should be changed to 5. The expressions in the third and forth line of Eq. (36) follow from the results for Appendix A.1. The fifth and the first term of the sixth line are obtained from Appendix A.2. Finally, the last term in Eq. (36) corresponds to the ultrasoft-potential running discussed in Appendix A.5.

Appendix B: Analytical result for the NNLL contribution to c_s

The analytical results for A_i and $f_i(z)$ of Eq. (19) read

$$\begin{aligned}
f_1(z) &= z^{3\beta_0-2C_A} {}_3F_2\left(1, 3 - \frac{2C_A}{\beta_0}, 3 - \frac{2C_A}{\beta_0}, 4 - \frac{2C_A}{\beta_0}, 4 - \frac{2C_A}{\beta_0}, \frac{z^{\beta_0}}{2}\right), \\
f_2(z) &= z^{3\beta_0-2C_A} {}_2F_1\left(3 - \frac{2C_A}{\beta_0}, 1, 4 - \frac{2C_A}{\beta_0}, \frac{z^{\beta_0}}{2}\right), \quad f_3(z) = z^{2\beta_0-(25C_A)/6}, \\
f_4(z) &= z^{2\beta_0-4C_A}, \quad f_5(z) = z^{2\beta_0-3C_A}, \quad f_6(z) = z^{2\beta_0-2C_A}, \quad f_7(z) = z^{2\beta_0-C_A}, \\
f_8(z) &= z^{\beta_0-(13C_A)/6}, \quad f_9(z) = z^{\beta_0-2C_A}, \quad f_{10}(z) = z^{\beta_0}, \quad f_{11}(z) = \ln(z), \\
f_{12}(z) &= \ln^2(z), \quad f_{13}(z) = \ln(2 - z^{\beta_0}), \quad f_{14}(z) = z^{2\beta_0-2C_A} \ln(2 - z^{\beta_0}), \\
f_{15}(z) &= z^{\beta_0} \ln(2 - z^{\beta_0}), \quad f_{16}(z) = z^{2\beta_0} \ln(2 - z^{\beta_0}), \quad f_{17}(z) = 1, \\
f_{18}(z) &= z^{2\beta_0}, \quad f_{19}(z) = \text{Li}_2\left(z_0^{\beta}/2\right). \tag{37}
\end{aligned}$$

$$\begin{aligned}
A_1 &= \frac{C_F^3(-2C_A^2 - 6C_AC_F - 4C_F^2)(C_A - 8n_lT_F)}{3(5C_A - 4n_lT_F)(9C_A - 4n_lT_F)^2(2C_A - n_lT_F)}, \\
A_2 &= -\frac{C_F^3(C_A^2 + 3CAC_F + 2C_F^2)(C_A - 8n_lT_F)}{4(5C_A - 4n_lT_F)(9C_A - 4n_lT_F)(2C_A - n_lT_F)^2}, \\
A_3 &= -C_F^4n_lT_F \frac{(3840C_A + 6144C_F)(-C_A + 8n_lT_F)}{13C_A(-5C_A + 4n_lT_F)(-9C_A + 8n_lT_F)(-19C_A + 16n_lT_F)^2}, \\
A_4 &= -3C_F^4 \frac{(23C_A - 4n_lT_F)(C_A + 4n_lT_F)}{8(5C_A - 4n_lT_F)^4}, \\
A_5 &= \frac{3CAC_F^3}{(13C_A - 8n_lT_F)^2}, \\
A_6 &= \frac{C_F^2}{\pi^2} \left[C_F \left(\frac{3n_lT_F(1009C_A^3 - 48C_A^2n_lT_F - 720CAC_Fn_l^2T_F^2 + 256n_l^3T_F^3)}{32(5C_A - 4n_lT_F)(11C_A - 4n_lT_F)^2(2C_A - n_lT_F)^2} \right) \right. \\
&\quad \left. + \frac{5975C_A^5 - 37478C_A^4n_lT_F + 22592C_A^3n_l^2T_F^2 + 18080C_A^2n_l^3T_F^3 - 17408CAC_Fn_l^4T_F^4 + 3584n_l^5T_F^5}{144(5C_A - 4n_lT_F)(11C_A - 4n_lT_F)^2(2C_A - n_lT_F)^2} \right] \\
&\quad + C_F^2 \left(\frac{-C_A^2}{16(2C_A - n_lT_F)^2} \right) + C_F^3 \left(\frac{-3CAC_A(11C_A - 16n_lT_F)}{16(5C_A - 4n_lT_F)(2C_A - n_lT_F)^2} \right)
\end{aligned}$$

$$\begin{aligned}
& + C_F^4 \left(\frac{3(1742C_A^2 - 1697C_A n_l T_F + 368n_l^2 T_F^2)}{104(5C_A - 4n_l T_F)(11C_A - 4n_l T_F)(2C_A - n_l T_F)^2} \right) \\
& + C_F^5 \left(\frac{3(13C_A - 32n_l T_F)(C_A - 8n_l T_F)}{104C_A(5C_A - 4n_l T_F)(11C_A - 4n_l T_F)(2C_A - n_l T_F)^2} \right), \\
A_7 &= C_F^3 \left(\frac{12C_A}{(19C_A - 8n_l T_F)^2} \right) + C_F^4 \left(\frac{-36}{(19C_A - 8n_l T_F)^2} \right), \\
A_8 &= C_F^4 n_l T_F \left(\frac{34560C_A + 55296C_F}{13(9C_A - 8n_l T_F)^3(5C_A - 4n_l T_F)} \right), \\
A_9 &= \frac{1}{\pi^2} \left[C_F^2 \left(\frac{-2C_A(C_A - 8n_l T_F)(397C_A^2 - 385C_A n_l T_F + 100n_l^2 T_F^2)}{3(5C_A - 4n_l T_F)^2(11C_A - 4n_l T_F)^2} \right) \right. \\
& \quad \left. + C_F^3 \left(\frac{-2(C_A - 8n_l T_F)(121C_A^2 - 70C_A n_l T_F + 16n_l^2 T_F^2)}{(5C_A - 4n_l T_F)^2(11C_A - 4n_l T_F)^2} \right) \right] \\
& + C_F^4 \left(\frac{36C_A(501C_A^3 + 706C_A^2 n_l T_F - 1480C_A n_l^2 T_F^2 + 448n_l^3 T_F^3)}{(9C_A - 8n_l T_F)(5C_A - 4n_l T_F)^4(11C_A - 4n_l T_F)} \right) \\
& + C_F^5 \left(\frac{-72(C_A - 8n_l T_F)(3C_A + 8n_l T_F)}{(9C_A - 8n_l T_F)(5C_A - 4n_l T_F)^3(11C_A - 4n_l T_F)} \right) \\
& + \frac{1}{\pi^2} \ln \left(\frac{\nu_h^2}{m_q^2} \right) C_F^2 \left(\frac{-2C_A(C_A - 8n_l T_F)}{2(5C_A - 4n_l T_F)^2} \right), \\
A_{10} &= -\frac{C_F^2}{\pi^2} \left(\frac{C_A(35C_A^2 - 164C_A n_l T_F + 80n_l^2 T_F^2 + 108C_F n_l T_F)}{2(5C_A - 4n_l T_F)(11C_A - 4n_l T_F)^2} \right) + C_F^2 \left(\frac{54C_A^3}{(11C_A - 4n_l T_F)^3} \right) \\
& + C_F^3 \left(\frac{108C_A^2(5C_A + 4n_l T_F)}{(5C_A - 4n_l T_F)(11C_A - 4n_l T_F)^3} \right) + C_F^4 \left(\frac{108C_A(533C_A + 38n_l T_F)}{13(5C_A - 4n_l T_F)(11C_A - 4n_l T_F)^3} \right) \\
& + C_F^5 \left(\frac{216(221C_A - 32n_l T_F)}{13(5C_A - 4n_l T_F)(11C_A - 4n_l T_F)^3} \right), \\
A_{11} &= \frac{1}{\pi^2} \left[C_F^3 \left(\frac{32C_A^2 - 89C_A n_l T_F + 32n_l^2 T_F^2}{4(5C_A - 4n_l T_F)(2C_A - n_l T_F)} \right) \right. \\
& \quad \left. + C_F^2 \left(\frac{-43C_A^3 - 120C_A^2 T_F + 40C_A^2 n_l T_F + 156C_A n_l T_F^2 - 16C_A n_l^2 T_F^2 - 48n_l^2 T_F^3}{6(5C_A - 4n_l T_F)(2C_A - n_l T_F)} \right) \right] \\
& + C_F^2 \left(\frac{-(C_A^2(59C_A^2 - 2C_A n_l T_F - 16n_l^2 T_F^2))}{6(11C_A - 4n_l T_F)^2(2C_A - n_l T_F)} \right) \\
& + \frac{C_F^3}{6(13C_A - 8n_l T_F)(19C_A - 8n_l T_F)(5C_A - 4n_l T_F)(9C_A - 4n_l T_F)} \\
& \quad \times \frac{1}{(11C_A - 4n_l T_F)^2(2C_A - n_l T_F)} \left(3C_A(9C_A - 4n_l T_F)(263641C_A^5 - 919114C_A^4 n_l T_F \right. \\
& \quad \left. + 1071256C_A^3 n_l^2 T_F^2 - 556448C_A^2 n_l^3 T_F^3 + 131456C_A n_l^4 T_F^4 - 11264n_l^5 T_F^5) \right. \\
& \quad \left. + 8C_A^2(C_A - 8n_l T_F)(13C_A - 8n_l T_F)(19C_A - 8n_l T_F) \right)
\end{aligned}$$

$$\begin{aligned}
& \times (11C_A - 4n_l T_F)^2 {}_2F_1(1, 1, 4 - (2C_A)/\beta_0, -1) \Big) \\
& + \frac{C_F^4}{2(19C_A - 16n_l T_F)(9C_A - 8n_l T_F)^2(19C_A - 8n_l T_F)(5C_A - 4n_l T_F)^3} \\
& \times \frac{1}{(9C_A - 4n_l T_F)(11C_A - 4n_l T_F)^2(2C_A - n_l T_F)} \left(-((9C_A - 4n_l T_F)(3565164294C_A^9 \right. \\
& - 13850749863C_A^8n_l T_F + 20837783628C_A^7n_l^2 T_F^2 - 13367118064C_A^6n_l^3 T_F^3 \\
& - 187327680C_A^5n_l^4 T_F^4 + 5932724736C_A^4n_l^5 T_F^5 - 3985068032C_A^3n_l^6 T_F^6 \\
& + 1224376320C_A^2n_l^7 T_F^7 - 176160768C_A n_l^8 T_F^8 + 8388608n_l^9 T_F^9)) \\
& + 8C_A(19C_A - 16n_l T_F)(C_A - 8n_l T_F)(9C_A - 8n_l T_F)^2(19C_A - 8n_l T_F) \\
& \times (5C_A - 4n_l T_F)^2(11C_A - 4n_l T_F)^2 {}_2F_1(1, 1, 4 - (2C_A)/\beta_0, -1) \Big) \\
& + \frac{C_F^5}{3(19C_A - 16n_l T_F)(9C_A - 8n_l T_F)^2(5C_A - 4n_l T_F)^2(9C_A - 4n_l T_F)} \\
& \times \frac{1}{(11C_A - 4n_l T_F)^2(2C_A - n_l T_F)} \left(-3(9C_A - 4n_l T_F)(9786501C_A^6 - 23721912C_A^5n_l T_F \right. \\
& + 22193456C_A^4n_l^2 T_F^2 - 11489920C_A^3n_l^3 T_F^3 + 4389888C_A^2n_l^4 T_F^4 \\
& - 1171456C_A n_l^5 T_F^5 + 131072n_l^6 T_F^6) \\
& + 8(19C_A - 16n_l T_F)(C_A - 8n_l T_F)(9C_A - 8n_l T_F)^2 \\
& \times (5C_A - 4n_l T_F)(11C_A - 4n_l T_F)^2 {}_2F_1(1, 1, 4 - (2C_A)/\beta_0, -1) \Big) \\
& + \ln(2) \left\{ \frac{2T_F C_F^2}{\pi^2} + C_F^2 \left(\frac{24C_A^3}{(11C_A - 4n_l T_F)^2} \right) + C_F^3 \left(\frac{576C_A^3}{(5C_A - 4n_l T_F)(11C_A - 4n_l T_F)^2} \right) \right. \\
& \left. + C_F^4 \left(\frac{1728C_A^2}{(5C_A - 4n_l T_F)(11C_A - 4n_l T_F)^2} \right) + C_F^5 \left(\frac{1152C_A}{(5C_A - 4n_l T_F)(11C_A - 4n_l T_F)^2} \right) \right\} \\
& + \frac{1}{\pi^2} \ln \left(\frac{\nu_h^2}{m_q^2} \right) C_F^2 \left(\frac{-C_A(5C_A - 4n_l T_F)(11C_A - 4n_l T_F)}{2(5C_A - 4n_l T_F)^2} \right), \\
A_{12} & = C_F^4 \left(\frac{-72C_A^2(48C_A^2 - 59C_A n_l T_F + 16n_l^2 T_F^2) - 36C_A C_F(3C_A + 8n_l T_F)(5C_A - 4n_l T_F)}{(9C_A - 8n_l T_F)(5C_A - 4n_l T_F)^2(11C_A - 4n_l T_F)} \right), \\
A_{13} & = C_F^2 \left(\frac{36C_A^3}{(11C_A - 4n_l T_F)^3} \right) + C_F^3 \left(\frac{(3456(C_A^2 + 2C_F^2) + 10368C_A C_F)C_A(2C_A - n_l T_F)^2}{2(5C_A - 4n_l T_F)(11C_A - 4n_l T_F)^3(2C_A - n_l T_F)^2} \right), \\
A_{14} & = -C_F^3 \left(\frac{(3C_A^2 + 9C_A C_F + 6C_F^2)(C_A - 8n_l T_F)(11C_A - 4n_l T_F)^2}{2(5C_A - 4n_l T_F)(11C_A - 4n_l T_F)^3(2C_A - n_l T_F)^2} \right), \\
A_{15} & = -C_F^3 \left(\frac{(1728C_A^2 + 5184C_A C_F + 3456C_F^2)C_A(2C_A - n_l T_F)^2}{2(5C_A - 4n_l T_F)(11C_A - 4n_l T_F)^3(2C_A - n_l T_F)^2} \right), \\
A_{16} & = \frac{-9C_A^3 C_F^2}{(11C_A - 4n_l T_F)^3}, \\
A_{17} & = \frac{1}{\pi^2} \left[C_F^2 \left(\frac{1}{144(5C_A - 4n_l T_F)^2(11C_A - 4n_l T_F)^2(2C_A - n_l T_F)^2} \right. \right.
\end{aligned}$$

$$\begin{aligned}
& \times (172973C_A^6 - 1635462C_A^5n_lT_F + 2956992C_A^4n_l^2T_F^2 - 2335616C_A^3n_l^3T_F^3 \\
& + 940032C_A^2n_l^4T_F^4 - 187392C_A n_l^5T_F^5 + 14336n_l^6T_F^6) \Big) \\
& + C_F^3 \left(\frac{1}{32(5C_A - 4n_lT_F)^2(11C_A - 4n_lT_F)^2(2C_A - n_lT_F)^2} \right. \\
& \times (30976C_A^5 - 277279C_A^4n_lT_F + 371548C_A^3n_l^2T_F^2 - 200144C_A^2n_l^3T_F^3 \\
& + 50240C_A n_l^4T_F^4 - 5120n_l^5T_F^5) \Big) \\
& + C_F^2 \left(\frac{-(C_A^2(2701C_A^3 - 2580C_A^2n_lT_F + 480C_A n_l^2T_F^2 + 64n_l^3T_F^3))}{16(11C_A - 4n_lT_F)^3(2C_A - n_lT_F)^2} \right) \\
& - \left(\frac{3C_A C_F^3}{16(13C_A - 8n_lT_F)^2(19C_A - 8n_lT_F)^2(5C_A - 4n_lT_F)(11C_A - 4n_lT_F)^3(2C_A - n_lT_F)^2} \right. \\
& \times (251269951C_A^8 + 767113748C_A^7n_lT_F - 3841834880C_A^6n_l^2T_F^2 + 5696836928C_A^5n_l^3T_F^3 \\
& - 4303456256C_A^4n_l^4T_F^4 + 1851312128C_A^3n_l^5T_F^5 - 454406144C_A^2n_l^6T_F^6 \\
& + 58130432C_A n_l^7T_F^7 - 2883584n_l^8T_F^8) \Big) \\
& - \left(\frac{3C_F^4}{8(19C_A - 16n_lT_F)^2(9C_A - 8n_lT_F)^3(19C_A - 8n_lT_F)^2(5C_A - 4n_lT_F)^4} \right. \\
& \frac{1}{(11C_A - 4n_lT_F)^3(2C_A - n_lT_F)^2} (900867787121646C_A^{14} - 6198841921859001C_A^{13}n_lT_F \\
& + 19119275729072316C_A^{12}n_l^2T_F^2 - 34644247240650784C_A^{11}n_l^3T_F^3 \\
& + 40320030084122112C_A^{10}n_l^4T_F^4 - 30355280730121984C_A^9n_l^5T_F^5 \\
& + 13082614024074240C_A^8n_l^6T_F^6 - 558681493807104C_A^7n_l^7T_F^7 \\
& - 3412540371369984C_A^6n_l^8T_F^8 + 2548850603065344C_A^5n_l^9T_F^9 \\
& - 1019296780124160C_A^4n_l^{10}T_F^{10} + 251825139744768C_A^3n_l^{11}T_F^{11} \\
& - 37363262685184C_A^2n_l^{12}T_F^{12} + 2860448219136C_A n_l^{13}T_F^{13} - 68719476736n_l^{14}T_F^{14}) \Big) \\
& - \left(\frac{3C_F^5}{8(19C_A - 16n_lT_F)^2(9C_A - 8n_lT_F)^3(5C_A - 4n_lT_F)^3(11C_A - 4n_lT_F)^3(2C_A - n_lT_F)^2} \right. \\
& \times (250339248081C_A^{10} - 1197788138208C_A^9n_lT_F + 2595380074848C_A^8n_l^2T_F^2 \\
& - 3536482592256C_A^7n_l^3T_F^3 + 3565032448256C_A^6n_l^4T_F^4 - 2818753511424C_A^5n_l^5T_F^5 \\
& + 1679893954560C_A^4n_l^6T_F^6 - 692836106240C_A^3n_l^7T_F^7 + 178875531264C_A^2n_l^8T_F^8 \\
& - 24964497408C_A n_l^9T_F^9 + 1342177280n_l^{10}T_F^{10}) \Big) \\
& + \pi^2 \left[C_F^2 \left(\frac{6C_A^3}{(11C_A - 4n_lT_F)^3} \right) + C_F^3 \left(\frac{144C_A^3}{(5C_A - 4n_lT_F)(11C_A - 4n_lT_F)^3} \right) \right. \\
& \left. + C_F^4 \left(\frac{432C_A^2}{(5C_A - 4n_lT_F)(11C_A - 4n_lT_F)^3} \right) + C_F^5 \left(\frac{288C_A}{(5C_A - 4n_lT_F)(11C_A - 4n_lT_F)^3} \right) \right]
\end{aligned}$$

$$\begin{aligned}
& + \ln^2(2) \left\{ C_F^2 \left(\frac{-36C_A^3}{(11C_A - 4n_l T_F)^3} \right) + \frac{-864C_A^3 C_F^3 - 2592C_A^2 C_F^4 - 1728C_A C_F^5}{(5C_A - 4n_l T_F)(11C_A - 4n_l T_F)^3} \right\} \\
& + {}_2F_1 \left(1, 1, 4 - \frac{2C_A}{\beta_0}, -1 \right) \left\{ C_F^3 \left(\frac{C_A^2(C_A - 8n_l T_F)}{2(5C_A - 4n_l T_F)(9C_A - 4n_l T_F)(2C_A - n_l T_F)^2} \right) \right. \\
& + C_F^4 \left(\frac{3C_A(C_A - 8n_l T_F)}{2(5C_A - 4n_l T_F)(9C_A - 4n_l T_F)(2C_A - n_l T_F)^2} \right) \\
& \left. + C_F^5 \left(\frac{C_A - 8n_l T_F}{(5C_A - 4n_l T_F)(9C_A - 4n_l T_F)(2C_A - n_l T_F)^2} \right) \right\} \\
& + {}_3F_2 \left(1, 3 - \frac{2C_A}{\beta_0}, 3 - \frac{2C_A}{\beta_0}, 4 - \frac{2C_A}{\beta_0}, 4 - \frac{2C_A}{\beta_0}, \frac{1}{2} \right) \\
& \times \left[C_F^3 \left(\frac{2C_A^2(C_A - 8n_l T_F)}{3(5C_A - 4n_l T_F)(9C_A - 4n_l T_F)^2(2C_A - n_l T_F)} \right) \right. \\
& + C_F^4 \left(\frac{2C_A(C_A - 8n_l T_F)}{(5C_A - 4n_l T_F)(9C_A - 4n_l T_F)^2(2C_A - n_l T_F)} \right) \\
& \left. + C_F^5 \left(\frac{4(C_A - 8n_l T_F)}{3(5C_A - 4n_l T_F)(9C_A - 4n_l T_F)^2(2C_A - n_l T_F)} \right) \right] \\
& + \frac{1}{\pi^2} \ln \left(\frac{\nu_h^2}{m_q^2} \right) C_F^2 \left(\frac{C_A(C_A - 8n_l T_F)}{(5C_A - 4n_l T_F)^2} \right), \\
A_{18} & = C_F^2 \left(\frac{9C_A^3}{(11C_A - 4n_l T_F)^3} \right) + C_F^4 \left(\frac{-3}{8(11C_A - 4n_l T_F)^2} \right), \\
A_{19} & = C_F^2 \left(\frac{-72C_A^3}{(11C_A - 4n_l T_F)^3} \right) + \frac{-1728C_A^3 C_F^3 - 5184C_A^2 C_F^4 - 3456C_A C_F^5}{(5C_A - 4n_l T_F)(11C_A - 4n_l T_F)^3}. \tag{38}
\end{aligned}$$

Appendix C: $O(\alpha^4 \ln^2 \alpha)$ and $O(\alpha^5 \ln^3 \alpha)$ corrections to the ratio of ortho- and parapositronium decay rates

We can also obtain novel results for the ratio of the ortho- (oPs) and parapositronium (pPs) decay rates by considering the Abelian limit of the previous computation and taking into account the modifications of the NRQCD matching coefficients due to the annihilation terms. The series for the decay rates ratio reads

$$\begin{aligned}
\frac{\Gamma(oPs \rightarrow 3\gamma)}{\Gamma(pPs \rightarrow 2\gamma)} & = \frac{4(\pi^2 - 9)}{9\pi} \alpha \left\{ 1 + \left(5 - \frac{\pi^2}{4} + A_o \right) \frac{\alpha}{\pi} + \frac{7}{3} \alpha^2 \ln \alpha \right. \\
& + \left[\left(5 - \frac{\pi^2}{4} \right)^2 + \left(5 - \frac{\pi^2}{4} \right) A_o + B_o - B_p \right] \left(\frac{\alpha}{\pi} \right)^2 \\
& \left. - \left[-\frac{73}{9} - \frac{7 A_o}{3} + \frac{7 \pi^2}{12} + 2 \log(2) \right] \frac{\alpha^3}{\pi} \ln \alpha \right\}
\end{aligned}$$

$$+ \frac{83}{36} \alpha^4 \ln^2 \alpha - \frac{7}{6\pi} \alpha^5 \ln^3 \alpha + \dots \} , \quad (39)$$

where $A_o = 10.286606(10)$, $B_o = 44.87(26)$ and $B_p = 5.1243(33)$. The first four correction terms in the curly brackets can be extracted from known results (see *e.g.* [50]). The last two terms are our new results.

References

- [1] T. Appelquist and H.D. Politzer, Phys. Rev. Lett. 34 (1975) 43.
- [2] W.E. Caswell and G.P. Lepage, Phys. Lett. B 167 (1986) 437.
- [3] G.T. Bodwin, E. Braaten, and G.P. Lepage, Phys. Rev. D 51 (1995) 1125; Erratum *ibid.* 55 (1997) 5853.
- [4] K. Hagiwara *et al.*, Phys. Rev. D 66 (2002) 010001.
- [5] M. Martinez and R. Miquel, Eur. Phys. J. C 27 (2003) 49.
- [6] W. Kwong, P.B. Mackenzie, R. Rosenfeld, and J.L. Rosner, Phys. Rev. D 37 (1988) 3210, and references therein.
- [7] J.H. Kühn, A.A. Penin, and A.A. Pivovarov, Nucl. Phys. B 534 (1998) 356.
- [8] A. Czarnecki and K. Melnikov, Phys. Rev. Lett. 80 (1998) 2531.
- [9] M. Beneke, A. Signer, and V.A. Smirnov, Phys. Rev. Lett. 80 (1998) 2535.
- [10] A.H. Hoang and T. Teubner, Phys. Rev. D 58 (1998) 114023.
- [11] A.A. Penin and A.A. Pivovarov, Phys. Lett. B 435 (1998) 413; Nucl. Phys. B 549 (1999) 217.
- [12] K. Melnikov and A. Yelkhovsky, Phys. Rev. D 59 (1999) 114009.
- [13] A.A. Penin and A.A. Pivovarov, Nucl. Phys. B 550 (1999) 375; Yad. Fiz. 64 (2001) 323 [Phys. Atom. Nucl. 64 (2001) 275].
- [14] A. Czarnecki and K. Melnikov, Phys. Rev. D 65 (2002) 051501; Phys. Lett. B 519 (2001) 212.
- [15] A.H. Hoang, A.V. Manohar, I.W. Stewart, and T. Teubner, Phys. Rev. Lett. 86 (2001) 1951.
- [16] A. Pineda, Phys. Rev. D 65 (2002) 074007; Phys. Rev. D 66 (2002) 054022.
- [17] A.H. Hoang and I.W. Stewart, Phys. Rev. D 67 (2003) 114020.

- [18] A.H. Hoang, Phys. Rev. D 69 (2004) 034009.
- [19] G. Källen and A. Sarby, K. Dan. Vidensk. Selsk. Mat.-Fis. Medd. 29, N17 (1955) 1.
- [20] I. Harris and L.M. Brown, Phys. Rev. 105 (1957) 1656.
- [21] A. Pineda and J. Soto, Nucl. Phys. Proc. Suppl. 64 (1998) 428.
- [22] B.A. Kniehl and A.A. Penin, Nucl. Phys. B 563 (1999) 200.
- [23] N. Brambilla, A. Pineda, J. Soto, and A. Vairo, Nucl. Phys. B 566 (2000) 275.
- [24] A. Pineda and J. Soto, Phys. Lett. B 420 (1998) 391; Phys. Rev. D 59 (1999) 016005.
- [25] A. Czarnecki, K. Melnikov, and A. Yelkhovsky, Phys. Rev. A 59 (1999) 4316.
- [26] B.A. Kniehl, A.A. Penin, V.A. Smirnov, and M. Steinhauser, Phys. Rev. D 65 (2002) 091503; Nucl. Phys. B 635 (2002) 357.
- [27] M. Beneke and V.A. Smirnov, Nucl. Phys. B 522 (1998) 321.
- [28] V.A. Smirnov, *Applied Asymptotic Expansions in Momenta and Masses* (Springer-Verlag, Heidelberg, 2001).
- [29] B.A. Kniehl, A.A. Penin, V.A. Smirnov, and M. Steinhauser, Phys. Rev. Lett. 90 (2003) 212001; Erratum *ibid.* 91 (2003) 139903.
- [30] M.E. Luke, A.V. Manohar, and I.Z. Rothstein, Phys. Rev. D 61 (2000) 074025.
- [31] B.A. Kniehl and A.A. Penin, Nucl. Phys. B 577 (2000) 197.
- [32] B.A. Kniehl and A.A. Penin, Phys. Rev. Lett. 85 (2000) 1210; Erratum *ibid.* 85 (2000) 3065; Phys. Rev. Lett. 85 (2000) 5094.
- [33] R.J. Hill and G.P. Lepage, Phys. Rev. D 62 (2000) 111301.
- [34] K. Melnikov and A. Yelkhovsky, Phys. Rev. D 62 (2000) 116003.
- [35] B.A. Kniehl, A.A. Penin, A. Pineda, V.A. Smirnov, and M. Steinhauser, DESY-03-172, TTP-03-40, UB-ECM-PF-03-28, hep-ph/0312086, to appear in Phys. Rev. Lett.
- [36] A.A. Penin, A. Pineda, V.A. Smirnov, and M. Steinhauser, DESY 04-042, TTP04-06, UB-ECM-PF-04-05, hep-ph/0403080, to appear in Phys. Lett. B.
- [37] A. V. Manohar and I. W. Stewart, Phys. Rev. D **62**, 014033 (2000).
- [38] A.A. Penin and M. Steinhauser, Phys. Lett. B 538 (2002) 335.

- [39] M.B. Voloshin, Nucl. Phys. B 154 (1979) 365; Yad. Fiz. 36 (1982) 247 [Sov. J. Nucl. Phys. 36 (1982) 143].
- [40] H. Leutwyler, Phys. Lett. B 98 (1981) 447.
- [41] S. Titard and F.J. Ynduráin, Phys. Rev. D 51 (1995) 6348.
- [42] A. Pineda, Nucl. Phys. B 494 (1997) 213.
- [43] A. Pineda, Acta Phys. Polon. B 34 (2003) 5295.
- [44] E. Braaten and Y.Q. Chen, Phys. Rev. D 57 (1998) (1998) 4236; Erratum *ibid.* D 59 (1999) 079901.
- [45] Y. Sumino, Phys. Rev. D 65 (2002) 054003; S. Recksiegel and Y. Sumino Phys. Rev. D 65 (2002) 054018; A. Pineda, J. Phys. G 29 (2003) 371; T. Lee, Phys. Rev. D 67 (2003) 014020.
- [46] A.V. Manohar, Phys. Rev. D 56 (1997) 230.
- [47] N. Brambilla, A. Pineda, J. Soto, and A. Vairo, Phys. Lett. B 470 (1999) 215.
- [48] A.V. Manohar and I.W. Stewart, Phys. Rev. Lett. 85 (2000) 2248.
- [49] K. Pachucki, Phys. Rev. A 56 (1997) 297.
- [50] A.A. Penin, hep-ph/0308204, and references therein.